

Femtosecond Lasers for Eye Surgery, Scanning Technology, Clinical Applications, Optical Coherence Tomography (OCT) and Alternative Imaging Technology

Zahraa Saleem Ne'mah ^{†1}, Banin Wameedh Abd Al-Hussein ², Zahraa Abd Al-Amir Sha'een ³, Shifaa Hamid Muzal ⁴

1,2,3,4 University of Babylon, College of Science for Women, Department of Laser Physics, Iraq.

ABSTRACT:The field of ocular surgery has had a significant impact on medical laser technology throughout the last four decades, and the reverse is also true. Because the eye, cornea, lens, and vitreous body are optically transparent, it is much easier to deliver laser energy at visible and near infrared (NIR) wavelengths at different focal depths through these structures than through other types of tissue in the body. This allows for surgical interventions to take place without opening or mechanically entering the eye, which is a unique advantage of fs-Laser technology. Refractive corneal surgery, therapeutic cornea treatments, and lens surgery were the original applications of fs-lasers. Additional novel ophthalmic applications are also in the works. The most recent idea in laser systems is low pulse energy and high pulse frequency. This allows for thermal tissue cutting with few side effects since bigger numerical aperture focusing optics reduce the pulse energy needed for optical breakdown. In the field of ophthalmic surgery, fs-laser technology has developed into a highly accurate, dependable, and adaptable instrument during the last several decades. Ergonomic and sturdy systems have become standard equipment in contemporary operating theatres for eye surgery when coupled with ancillary technologies such as sterile eye docking systems, optical coherence tomography (OCT) imaging, rapid laser scanning, and sophisticated software. Global standards for fs-Laser-assisted cataract and corneal surgery are now rather high.

Keywords: Femtosecond Lasers, Scanning Technology, Optical Coherence Tomography (OCT), Imaging Technology

Corresponding Author:Zahraa Saleem Ne'mah ,University of Babylon, College of Science for Women, Department of Laser Physics, Iraq.

Copyright : © 2024 The Authors. Published by Vision Publisher. This is an open access article under the CC BY-NC-ND license (<https://creativecommons.org/licenses/by-nc-nd/4.0/>).

Introduction

Since its inception, ophthalmology has been at the forefront of medical laser use. Because it is transparent to both visible and near-infrared light, the human eye is one of the most easily accessible organs in the body, and optical techniques can be used to diagnose and treat nearly any ocular structure. In the late 80s, laser vision correction (LVC) was first developed. As a result of its high success rate, minimally invasive nature, and relative ease of procedure, laser-assisted in-situ keratomileusis (LASIK) has surpassed all other refractive surgical procedures in terms of

frequency of use. It has just been shown that some parts of LVC can use special light-matter interaction mechanisms that happen with femtosecond laser pulses. Improved methods of imaging the eye have been made possible by ongoing developments in microscopic imaging. Confocal laser scanning ophthalmoscopy, developed in the last ten years and based on the confocal imaging concept, offers a significant improvement in sensitivity and resolution over fundus cameras and slit lamp ophthalmoscopy for in vivo imaging of the cornea and retina. The distinct benefits of nonlinear multiphoton laser scanning microscopy, such as submicrometer resolution, high sensing depth, and minimised photon damage, have recently attracted the interest of cell biologists in living cell imaging. A new two-photon scanning laser ophthalmoscope (SLO) based on the multiphoton microscopy concept is currently the subject of active research. In addition to high-resolution in vitro microscopic imaging of excised retinal and corneal tissues, the two-photon SLO can also conduct in vivo ophthalmic imaging of the human eye's living retina and cornea. In the femtosecond time regime, laser-tissue interaction results in a very precise cut with almost no collateral damage. Because of this, amplified femtosecond pulse lasers will be promoted as a flexible, accurate, and minimally invasive surgical tool. Furthermore, the presentation covers a range of topics related to solid-state laser technology, including the fundamental physics involved in producing and amplifying femtosecond laser pulses. We compare the gold standard in LVC, the ArF excimer laser, with a real-world surgical laser system that is built for safe and dependable clinical use. Surgical operations, such as customised flap cutting, can benefit from optimised scanning strategies. We will next review the diagnostic uses of femtosecond lasers in the field of ophthalmology in Part 3. We recently used two-photon laser scanning microscopy to study the human eye's cornea and retina at submicron resolution, delving into their ultrastructures. Here, the ultra-structures of collagen fibrils in the cornea, sclera, and lamina cribrosa were characterised using second harmonic generation (SHG) imaging. Retinal pigment epithelial (RPE) cells have their morphology and spectra resolved using two-photon excited autofluorescence (TPEF) imaging.

Using a Laser on Tissue.

Displayed is a double-logarithmic graph containing the five most fundamental kinds of interactions. The applied power density, in W/cm^2 , is shown on the ordinate. In seconds, the exposure time is shown on the abscissa. The two diagonals display energy fluxes that are constant at $1 J/cm^2$ and $1000 J/cm^2$, correspondingly. Using this chart as a guide, we may approximately categorise the time scale as follows: photochemical interactions, which involve continuous waves or exposure lengths above 1 second; thermal interactions, which range from 1 second down to 1μ second; photo-ablation, which spans from 1μ second down to 1 nanosecond; and plasma-induced ablation and photo-disruption, which span less than 1 nanosecond. The energy densities are different in the second two, which is why they differ. In contrast to photo-disruption, which is mostly a mechanical action, plasma-induced ablation relies only on ionisation.

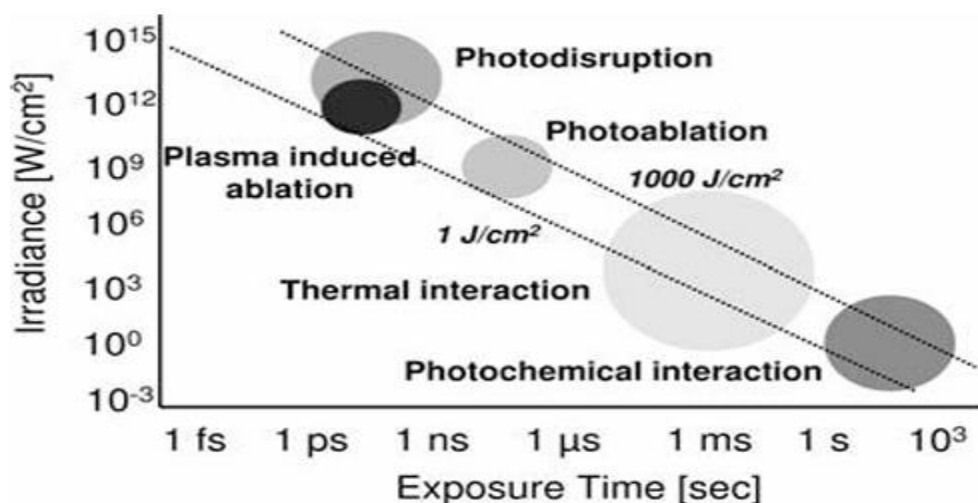


Figure 1. Laser–tissue interaction

The effects of pulsed laser radiation on many bulk materials, including metals, biological substances, and dielectrics, have been the subject of multiple investigations. Unlike the statistical behaviour of long-pulse interaction, short-pulse damage is often shown to be deterministic. The typical result is that the threshold fluence needed to cause material

damage scales with $\sqrt{\tau_p}$ for pulse durations τ_p between 100fs and 100 μ s. The fact that the thermal diffusion length similarly increases as $\sqrt{\tau_p}$ grows explains this. That is why it is possible to get higher energy densities with less energy diffusing into the bulk for a given pulse energy. A lot of research has gone into the effects of creating plasma in tissue via laser-induced avalanche ionisation. The two most essential mechanisms in ultrashort pulse laser-tissue interaction, plasma-mediated ablation and photo-disruption, are both influenced by this mechanism, which is called laser induced optical breakdown (LIOB). The tissue is illuminated with concentrated, extremely brief bursts of laser light. A micro-plasma is produced at the beam focus as a result of optical breakdown caused by exceedingly strong local field strengths compared to the electric field that binds valence electrons to their atoms. In the focal volume, there are significant pressure and temperature gradients because the produced plasma absorbs more energy from the laser pulse. Shock waves and cavitation bubbles are unintended consequences that result from plasma growth. An energy density of 40Jcm⁻² is necessary for LIOB on human corneal tissue with a pulse length of 200ps. Lowering the LIOB threshold below 1Jcm⁻² is achieved by utilising amplified 350fs pulses. Also decreased were the shock-wave radius and the size of the cavitation bubble. With careful selection of the laser parameters, the interaction between the tissue and the laser allows for a clean cut with little collateral damage. The versatility, precision, and lack of invasiveness of amplified femtosecond pulse lasers make them an attractive surgical tool. Pulses of extremely brief laser light can only ablate a tiny fraction of tissue at a time. Depending on the settings of the laser and the focusing strategy, ablation zones can be as tiny as a few micrometres or even smaller. By using the ablation effects of single ultrashort laser pulses in precise patterns, larger amounts of tissue can be eliminated. Consequently, the surgical treatment must also take into consideration the size of the gas bubbles, which is a critical parameter. It is not enough for subsequent laser pulses to just strike the gas bubbles produced by earlier pulses; other targets must also be targeted. Interactions between lasers and tissues with pulse lengths in the picosecond range or longer cause heating of the tissue by transferring a great deal of energy to the vibronic states of bulk molecules. Material degradation from melting and vaporisation is the most common in this time regime. Thermal diffusion increases the pulse energy needed for ablation within the focus and the collateral thermal damage by transferring energy out of the focal volume. When it comes to femtosecond irradiation, things are completely different. For example, because the contact periods are so brief, thermal coupling does not happen during plasma-mediated ablation of tissue with ultrashort laser pulses. Investigations into the underlying mechanisms of ultrafast laser tissue destruction have revealed the absence of substantial collateral thermal damage. Research has also shown that compared to longer pulses, ultrashort pulses achieve a plasma-mediated ablation threshold for dental enamel, corneal tissue, and brain tissue at lower fluences. To summarise, when designing pulsed medical laser systems and related surgical procedures, it is crucial to consider the influence of threshold fluence on pulse length. Smaller gas bubbles and less shock-wave phenomena are the results of using shorter laser pulses, which need lower pulse energy for ablation. On the other hand, self-focusing and self-phase-modulation are two undesirable nonlinear effects that ultrashort pulses can cause. For certain uses in ophthalmic surgery, such as corneal surgery, the pulse length range of 500-700 fs appears to be optimal. Next, we'll go over how surgeons might take use of intrastromal ablation and other advantages of ultraprecise tissue manipulation with the help of modern femtosecond laser technology. Concurrently, the laser system is engineered for regular use in the medical field.

Modern Technology in All-Solid-State Femtosecond Lasers

Compact and easy-to-use, femtosecond surgical lasers are necessary for real-world applications. Medical ultrafast lasers must also be inexpensive, self-maintaining or require little maintenance, have highly reproducible emission characteristics, and be turnkey in order to operate in a clinical setting and comply with regulatory requirements. However, there are a number of practical drawbacks to huge power laser systems, such as the complexity that comes with them, the instabilities that come with high power (electrical/optical) inputs, the hazards of optical damage, the cooling requirements, and mechanical stability. Small, long-lived semiconductor laser diodes supply the necessary optical energy to the femtosecond laser in directly diode-pumped solid-state lasers, which is one possible approach. A Nd:glass rod serves as the laser medium in our concept. Laser diode pumped Nd:glass lasers have demonstrated superiority over the routinely used Ti:Sapphire lasers in ocular surgical procedures. Nonlinear, intensity-dependent events are utilised to generate picosecond or femtosecond pulses. It all started with the Kerr lens mode locking (KLM) mechanism. But KLM usually doesn't start on its own and needs the laser cavity components to be perfectly aligned. Through the use of semiconductor saturable absorber mirrors and passive mode locking, a considerably more stable

pulse-forming mechanism was accomplished. Pulsed operation with a greater peak power of the laser is favoured by these intra cavity elements, which induce significant losses at low incident fluences and low losses at high incident fluences. Modularizing the laser system's pulse generating and amplification modules is a proven design strategy for providing the pulse energy needed by practical applications of short-pulse laser systems. One name for this setup is the "chirped pulse amplification" (CPA) system. One possible approach is to employ a tiny, precisely-controllable oscillator laser to produce a series of extremely brief pulses with little energy. A second stage would then amplify these pulses to levels where they may be put to good use. The lab setup of a femtosecond laser system for surgical applications and the viability of its clinical use in tissue studies were demonstrated in a collaborative study between the University of Heidelberg and 20/10 Perfect Vision. An Nd:glass oscillator is the first component of the system. The active laser medium receives its optical energy from semiconductor laser diodes using specialised optics. Semiconductor saturable absorber mirrors (SESAMs) generate pulses with a repetition rate of mega hertz that are sub 200 fs long and can reliably generate femtosecond pulses. In order to prevent distortion or damage to optical components during amplification, the output pulses of this oscillator laser must be stretched in time. In this case, we directly benefit from the wide spectrum that is linked to extremely brief pulses. The process of stretching involves spreading out the beam and then redistributing its spectral components in the time domain, a process known as chirp. An electro-optical crystal is used to couple the stretched pulses into the amplifier laser. Each time the pulse travels through the amplifier's active laser material, it acquires energy. After around 100 iterations, this building process reaches its maximal pulse energy. Pulse energy would inevitably start to decrease due to inevitable cavity losses once all extractable energy has been transmitted to the pulse. Consequently, the pulse is promptly removed from the amplifier once the build up maximum is reached. In a grating compression stage, the stretched and amplified pulses are recompressed to 500..900 fs. The original pulse duration cannot be entirely retrieved due to the limited amplification bandwidth of the laser active material. You can do tissue tests using near infrared pulses with energy of several μJ and a repetition rate of 1..10kHz after compression. It goes without saying that not every surgical procedure can benefit from ultrashort-pulse lasers. If you need to ablate material within tissue or in a fluid, or if you need to ablate a small amount of tissue without damaging other tissue sections, then ultrafast laser technology is the way to go. Bone and teeth, which are hard tissues with a low water content, have a reduced ablation efficiency and yet necessitate substantial tissue removal (often several cubic millimetres) in most surgical operations. One possible improvement for drilling into human teeth, though, is the use of extremely short bursts of laser light. It is possible to distinguish between ablated carious and healthy tissue by watching the LIOP-plasma emission spectra. In this way, the laser might be directed to drill precisely the smallest hole required for filling. There are a number of noticeable distinctions between the innovative femtosecond laser and the conventional ArF excimer laser used in the ophthalmic field. Because of the infrared emission wavelength and the extremely quick mechanisms of laser-tissue interaction, only the femtosecond laser can be utilised for intrastromal surgery.

A femtosecond laser's potential in ophthalmic surgery

The Q-switched Nd:YAG solid-state lasers were the first to be effectively utilised in ophthalmology as a short-pulsed laser. Because the cornea, lens, and vitreous body are completely see-through in the visible and near infrared spectrums (1064 and 532 nm, respectively), these instruments are ideal for use in the eye. Their pulse energies range from 0.3 to 10 mJ, and their durations are just a few nanoseconds (ns), making them ideal for usage in the eye. The combination of short pulse durations and strong internal focus of Nd:YAG laser pulses to spot sizes of a few microns results in extremely high intensities at the laser focus, exceeding 1011 W/cm².

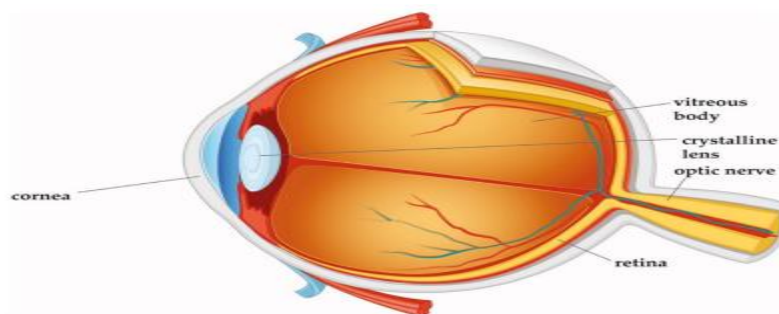


Figure 2: Cross-section of the eye. Cornea, crystalline lens, and vitreous body are transparent in the healthy eye. Copyright© Dardenne Clinic

Optical breakdown happens under these circumstances. As a first step, tissue molecules are ionised and free electrons are created through multi-photon absorption. The second phase involves accelerating these "seed" electrons by absorbing their photon energy. The process of electron ionisation via impact ionisation produces more free electrons once a certain number of photon absorptions have brought the electrons' kinetic energy to a high enough level. An avalanche effect can happen if the intensity of the laser beam is high enough to counteract electron losses. A plasma state of matter, consisting of a cloud of ions and free electrons, is generated at the laser focus when the extremely fast growing electron density surpasses values of about $10^{20}/\text{cm}^3$. For photons of any wavelength, this plasma is an excellent absorber. The plasma's temperature and energy density are therefore increased as it absorbs the majority of the remaining laser pulse. The energy initially carried by free electrons thermalizes within a few picoseconds (ps) to tens of ps, allowing the hot plasma to quickly recombine into a heated gas. Due to the confinement of the thermoelastic strains induced by the temperature rise, this period is significantly less than the acoustic transit time from the centre of the focus to the periphery of the plasma volume. The stress wave that is released in this geometrical arrangement must have compressive and tensile components in order to maintain momentum conservation. A cavitation bubble is created when the tensile stress wave is delivered with a density of pulses that is high enough to induce tissue fracture. Pressure waves can achieve shock wave speeds close to supersonic levels, depending on the energy of the pulse. Ethane, water vapour, and gases such as helium, oxygen, and methane are produced as the tissue within the focal volume evaporates almost instantly due to the high plasma temperature. Because of the subsequent gas pressure, the adjacent tissue is forced to move further away. When the pulse energy is greater than the threshold for laser-induced optical breakdown (LIOB), the maximum volume that the bubble can momentarily achieve scales with the pulse energy. Due to the inertia of the outwardly flowing material, the internal pressure of the expanding bubble can eventually fall below atmospheric pressure, causing the bubble to dynamically collapse. Another shock wave might be generated if the bubble bursts. Collectively, these effects are commonly known as "photodisruption" of tissues.

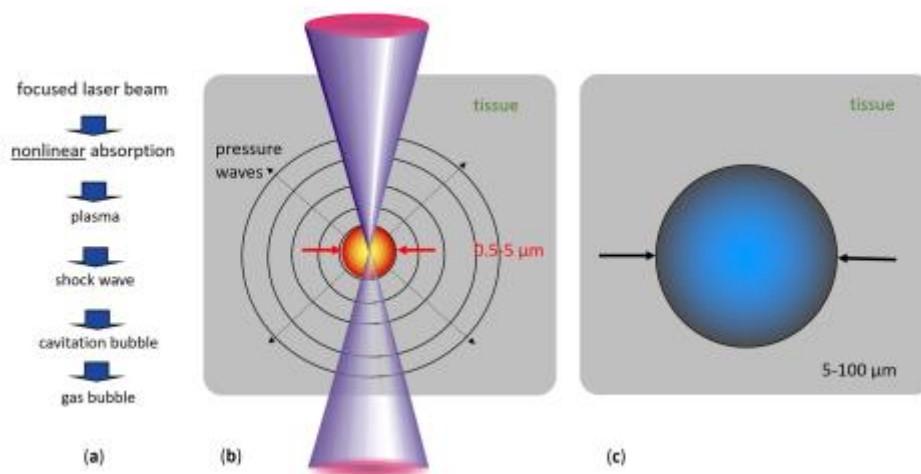


Figure 3. fs Pulse laser effects in tissue: (a) sequence of events, (b) plasma diameter range (red) and emitted pressure wave pattern (circles), and (c) range of possible cavitation bubble dimensions (pulse energy dependent)

The cavitation bubble radii and shock wave amplitudes at 1 mm distance from the focus are 1000-2000 μm and 100-500 bar, respectively, when using common ophthalmic Nd:YAG laser pulse energies. Because of these noticeable mechanical side effects, Nd:YAG lasers are not widely used. Shorter pulse ps (10–12 s) lasers had smaller mechanical side-effects when they were introduced, but they were still too big for sensitive activities like many ophthalmic applications. The use of Nd:YAG lasers in clinical ophthalmology is thus restricted by this.

Thermosecond lasers

A more recent development in solid-state laser technology are femtosecond (fs: 10⁻¹⁵ s) lasers. Their pulse duration is shorter than 1 ps, and they operate at near-infrared wavelengths, which are similar to Nd:YAG lasers. Due to the significantly lower threshold radiant exposure (J/cm²) for producing LIOB in tissue in the fs pulse duration regime compared to 10 ns, significantly lower pulse energies can be used to separate tissue. Afterwards, three-dimensional beam scanning systems employ high pulse frequencies ranging from fifteen kilohertz (kHz) to several megahertz (MHz) to produce continuous cut planes within the tissue by positioning several pulses closely together. The mechanical side effects of the LIOB are significantly reduced as a result of the decreased pulse energies. In comparison to ns pulses with energies in the mJ range, the cavitation bubbles produced by 300 fs pulses with 0.75 μJ energy had radii of just 45 μm in water, a difference of nearly two orders of magnitude. Concurrently, the pressure waves are significantly less intense, measuring just 1–5 bar at a distance of 1 mm. Since the aforementioned disruptive mechanical side effects of ns pulses are not present in this process, it is called "plasma-induced ablation". Furthermore, there is practically no thermal side effect of fs pulses on tissue.

Fs lasers that are modern and use low pulse energy and high pulse frequency

The pulse energy of the early fs lasers employed in ophthalmic surgery were approximately 10 μJ, which were relatively high. Two process parameters can be optimised to further lower pulse energies and their related side effects at a given wavelength: To begin, pulse length can be reduced; older fs lasers could produce pulses as long as 800 fs, while newer ones can only manage 200-300 fs. Additionally, by decreasing the size of the focal spot, we can decrease the focal volume of a Gaussian laser beam. This volume is determined by the axial extension, also known as the Rayleigh range ($z_R = \pi w_0^2 / \lambda$), and the beam waist $w_0 = f \lambda / \pi w_L$, where f is the lens's focal length, w_0 is the focus beam radius, and w_L is the focusing lens beam radius. To rephrase, the relation between the cube of the numerical aperture $NA = w_L / f$ and the focal volume of the focusing optics is inverse. The energy threshold for LIOB decreases as the numerical aperture NA increases, which in turn causes the focal spot to shrink. There are two practical ways to improve the NA: either move the focusing optics closer to the eye, which is more efficient but quickly becomes cumbersome and expensive, or increase the lens diameter of the optics. The majority of laser systems still use the initial technique, which was introduced to the market by IntraLaseTM in 2003. By adopting the second method, Ziemer Ophthalmic Systems was able to bring more compact laser focusing optics into closer proximity to the eye. As focusing optics, we used a short-focus lens from a microscope to accomplish this. This method has the potential to cut pulse energies by over a factor of 10. A small device was made possible by directing the laser beam to a handpiece that contained the focusing optics via an articulated mirror arm. The usage of the handpiece allowed for the utilisation of the laser beneath a surgical microscope, eliminating the necessity to relocate the patient during the procedure. In 2007, the first systems developed specifically for corneal surgery were introduced to the public. In comparison to more traditional systems, this one was smaller and lighter. Having wheels made it possible to move it around different buildings and even carry it in a small van between different clinics.

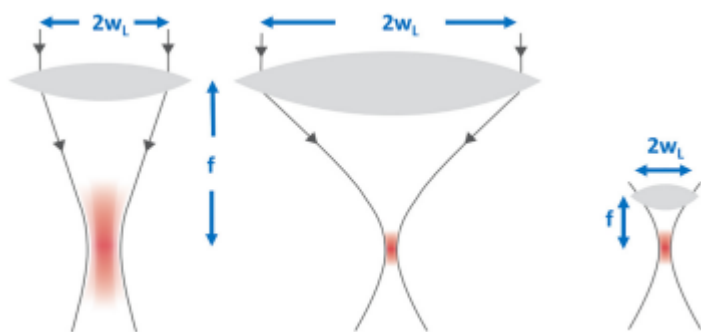


Figure 4. The focal volume of a Gaussian laser beam scales inversely to the cube of the numerical aperture $NA = w_L / f$ of the focusing lens. The larger the NA, the smaller the focal spot volume. Copyright© Ziemer Ophthalmic Systems.

Interaction between femtosecond lasers and tissues

There are seven critical laser parameters that dictate the process regime of ultrashort pulse laser-tissue interaction: Both the intensity of the pulse and its repetition rate - The time per pulse length of a wave - The numerical aperture (NA) of the lens used for focusing - Shape of the focus spot (Gaussian or non-Gaussian, generally devoid of aberrations) - Spatial pulse spacing, also known as pulse raster. The two classes of fs lasers perform different types of cutting depending on the aforementioned laser properties. High pulse energy lasers use mechanical forces applied by expanding bubbles to drive the cutting process. When the bubbles burst, they cause tissue damage at a wider radius than the plasma generated by the laser. Conversely, for plasma interaction zones that overlap spatially, spot separations lower than spot sizes are utilised in the low pulse energy group. The tissue within the plasma volume can be successfully separated by evaporation, eliminating the need for further mechanical ripping effects. The effective cutting speeds attained are comparable to those of the high energy laser group when high pulse frequencies (in the MHz range) are additionally employed. A distinctively smooth surface, with almost minimal damage to the surrounding tissue, is the result of tissue incisions accomplished by overlaying plasma interaction zones with low energy pulses. When it comes to refractive eye surgery, this is especially crucial for the accuracy of corneal incisions (also known as "flaps" and lenticular cuts) in humans. For further information, this regimen is also helpful when cutting other sensitive eye tissues during therapeutic cornea and cataract surgeries. To separate tissues in between the laser foci, high-energy pulses with a low pulse frequency largely use mechanical tearing. The levels of stress hormones discovered after laser treatments indicate that this ripping is followed by increased stress or possibly even injury to the surrounding tissue. Interactions with tissue are typically only caused by the fraction of a laser pulse's energy that is actually absorbed inside the tissue. The process of tissue dissection is aided solely by nonlinear absorbed energy. For fs pulses, this fraction of the total energy output is around 10–25%; nevertheless, it is quite process parameter dependent. Until the irradiance threshold for LIOB is reached in the centre of the focus, the first portion of a laser pulse is mainly transmitted since the transparent eye tissues have a very low linear absorption of the IR wavelengths (1030-1060 nm) employed in clinical fs lasers, approximately 0.1 cm⁻¹. Pulse energies just above the threshold can cause a diverging beam with rapidly falling irradiance to dissipate harmlessly, allowing more than half of the incident energy to be transmitted beyond the focus.

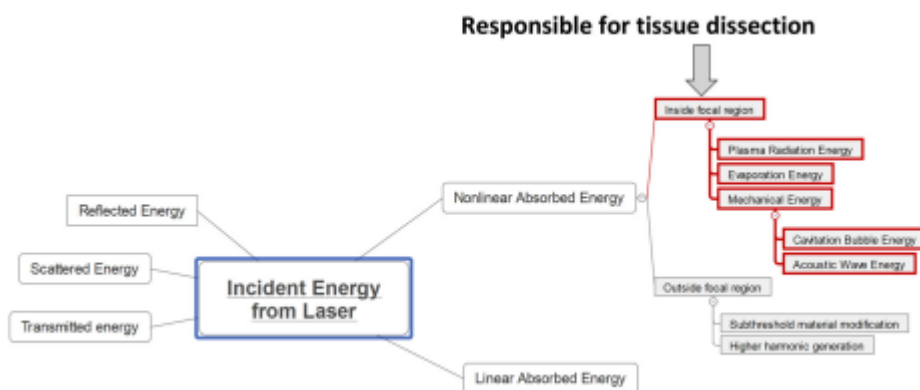


Figure 5: Redistribution of energy in a pulsed laser process for tissue dissection.

In ophthalmic practice, slightly opaque tissue can absorb and scatter laser radiation, reducing the amount of energy that reaches the laser focus. Higher pulse energies are needed, for instance, when laser cutting the cornea at scar-ridden areas compared to typical, clear cornea. The amount of energy lost as a result of scattering is proportional to the thickness of the material that the laser light must pass through on its way to the focus. Since corneal scars are just a few micrometres thick and can absorb up to ten percent of the incident energy, cutting through a cataract lens nucleus that is several millimetres thick results in a much greater energy loss. The produced plasma only reaches a significantly lower density when using fs Laser pulses with energies slightly higher than the LIOB threshold compared to pulses with high energies. As a result, following each laser pulse, relatively little thermal energy is delivered to the next tissue. This, along with the relatively low linear absorption, suggests that the mechanism is not thermal in nature. Only the most superficial area of a cut smaller than one micron (i.e., a cell) can show changes to the tissue that could be caused by a heat contact. This differs from previous regimes of laser-tissue interaction, where thermal effects have been either intentionally introduced or are present but undesirable. It is possible to characterise the laser process with an acceptable quantity of applied laser dose in those ranges. The interaction between fs lasers and tissues is not

adequately described by the incident or emitted energy in terms of total dosage. The regimes of low and high energies are equally affected by this. After 20 years of study and clinical application, we are unaware of any reports of thermal adverse effects associated with fs lasers that are clinically significant. Process parameters that cause mechanical effects are more crucial than a total dosage. To start with, the most important component of pulse energy is the portion that causes cavitation bubbles and shock waves, which may be felt even when the laser is far away. The mechanical impact on tissue layers close to the cut can be altered by adjusting the fs process regime, as opposed to the insignificant thermal effects. Researchers found that the lower pulse energy regime of nJ and μ J pulse energy fs-laser corneal cutting prevented cell injury and decreased inflammation reactions in the surrounding stroma tissue. A wide variety of pulse energies are available in today's flexible ophthalmic fs-laser systems, allowing for the application of tailored doses of pulse energy for different types of tissues and different geometric structures. Reducing gas production and mechanical side effects is possible by only applying the necessary amount of pulse energy, and nothing more.

Equipment necessary for ophthalmic fs-laser systems

The development of some essential ancillary technologies is also necessary for the realisation of feasible fs-laser systems for usage in clinical settings. Notable among these is the patient interface system, which assures a steady relative position during treatment by suctioning the eye into contact with the laser beam delivery system. Cuts can only be made at precise locations when additional imaging of tissue structures and laser beam scanning technologies have been utilised.

System for patient interface

A gantry with focusing optics is used by some laser systems to position the patient's head. For the patient's head to be able to move in and out, a working distance that is long enough is needed. Docking requires either the gantry or the patient support device to move. Alternative systems make use of an articulated arm that, at its tip, has a handpiece that contains focusing optics. It is possible to bring the optics quite near to the eye because of the flexible arm. During docking, the patient is kept immobile. "Patient interfaces" are the sterile, one-time-use components that make direct eye contact. Applanating interfaces, which have a curved or flat surface that touches the cornea directly, and so-called liquidoptics interfaces, which have a vacuum ring that contacts the sclera or outer cornea and a liquid-filled centre, are the two types that are used. With the use of liquid-optics interfaces, laser energy can be transmitted while the cornea maintains its original shape. Their primary usage is in the field of cataract surgery. By making mechanical contact, applanating interfaces stabilise the cornea position during surgery very efficiently. Because of the critical need of precisely locating intra-corneal cuts during refractive surgery, these procedures—which are marginally more invasive—are reserved for such cases. The docking contact's stability during laser emission is crucial. Cutting in the wrong planes is a risk that arises when there is a loss of touch. Consequently, lasers are programmed to detect when contact is lost and instantly cease output. This monitoring of vacuum levels is frequently enhanced by imaging of the eye's position, a feature known as eye tracking. It goes without saying that eye doctors keep a close check on their patients as well. Surgeons can also employ their physical dexterity to actively stabilise the laser handpiece as it comes into contact with the eye in the case of articulated arm laser systems. When patients inadvertently move during surgery, this can help keep the vacuum from escaping.

Optogenetics and complementary imaging methods

Some laser systems also offer depth ranging, in addition to integrated camera systems that give a frontal image of the eye. The optical technology known as optical coherence tomography (OCT) may produce images of structures within tissues, much like ultrasound, but with a resolution of 5-20 μ m, which is almost microscopic. In 1988, Adolf Fercher et al. documented the initial use of optical coherence tomography (OCT) in a biological context: measuring the axial length of the eye in a controlled laboratory setting. The first optical coherence tomography (OCT) devices for clinical usage relied on time domain (TD) OCT, a technique that involves mechanically adjusting the interferometer's reference arm length. Older devices could only do very slow 1D scans (A-scans) or, later, very tiny 2D scans because of the limitations of this technology. An innovation in optical coherence tomography (OCT) was the frequency-domain (or "Fourier domain") technique, which employed a spectrometer with a linear array of detectors rather than a single detector and maintained a constant reference arm length. In this scenario, the interference spectrum exhibits

periodic modulation due to variations in optical path length between the interferometer arms. It is possible to obtain full A-scans from the observed spectra at the detector array's frame rate using Fourier transformation. Published in 2002 was the first FD-OCT application to the eye. Subsequently, "swept-source" (SS) OCT emerged as a variant of frequency-domain OCT. In this setup, a spectrometer is replaced with a quick single-pixel detector and a tuneable light source that can be adjusted to sweep frequencies as seen by a saw-tooth frequency profile over time. The greater measurement ranges and shot-noise limited resolution are advantages of SS-OCT, which is an improved version of FD-OCT. Optical coherence tomography (OCT) was originally developed for use solely in examining the retina. Imaging the front portion of the eye has also been possible since the technology was refined in 1994. In order for cataract surgery laser systems to be practicable, it was necessary to be able to swiftly create high-resolution cross-section images of the lens, anterior chamber, and cornea. Though initially proposed by Zeiss, imaging-guided femtosecond laser surgery was initially demonstrated by H. Lubatschowski et al. After docking the laser interface to the eye, 3D optical coherence tomography scans are typically performed in most contemporary cataract fs-laser systems. An alternative approach, 3D confocal structured illumination with Scheimpflug imaging, is employed by the LENSARTM system. The imaging lens is positioned at an acceptable angle between the object and image planes in Scheimpflug imaging, which uses a tilted setup. When used in conjunction with a slit lamp, it enables high-resolution imaging of a tissue section at varying depths within the anterior portion of the eye, such as the cornea and lens all at once. A three-dimensional picture of the whole anterior segment can be obtained by turning this imaging apparatus around the eye's optical axis and then processing the pictures in software. Zeiss introduced the SLC, the first rotational video version with electronic image processing, while Topcon introduced the SL-45, the first commercial medical Scheimpflug camera. Cornea topographers and other diagnostic eye imaging devices now frequently employ the same idea. When it comes to seeing tissue borders in a less transparent environment (like corneal scarring), Scheimpflug technology isn't always up to snuff. It is feasible, however, to modify the lens fragmentation pattern in accordance with an estimated lens density derived from recorded local light scattering. Next, image processing software examines the acquired images, determining the tissue boundaries of interest, without relying on Scheimpflug or OCT technologies. The iris, front and back surfaces of the lens, and cornea are very important components of the eye.

Imaging apparatus

A medically required cut pattern inside the eye can only be achieved by arranging the individual laser spots in appropriate geometric patterns. Programmes direct scanning systems to place laser focuses in specific lines, planes, or even three-dimensional shapes, and they also compute these patterns. A combination of galvanometer-driven scanning mirrors and another device to adjust the focus position along the beam axis allows for two-dimensional optical scanning of the laser focus. On the other hand, rapid micro-scanning technology and mechanically displaced focusing optics with a smaller field diameter are also utilised for 3D focus location. The following is a sample of a cut pattern commonly used to create cornea flaps:

Medical uses

When Aron-Rosa first used short pulse lasers at near-IR wavelengths to treat posterior capsule opacification (PCO) following cataract surgery in 1979, she was the first to report this usage of these lasers in the field of ophthalmology. Ablation profiles revealed improved accuracy and less collateral damage when the pulse width of ultrashort-pulsed lasers was reduced from nano- to femtoseconds, as proven by Stern et al. in 1989. Also around this time, optical coherence tomography came out, allowing for non-invasive three-dimensional in vivo imaging with micrometer-level resolution in both the axial and lateral directions. These advancements finally enabled a wide range of therapy uses for these types of lasers within the area of ophthalmology, providing ocular surgeons with a tool for highly precise cutting and visual control through imaging. Increases in the numerical aperture and the pulse frequency of laser sources have led to improvements in laser focusing optics, which have further reduced collateral damage while enhancing precision. Launched in 2003, the IntraLaseTM FS was the first clinical fs-laser system for ophthalmology to get FDA approval. In refractive surgery known as laser in situ keratomileusis (LASIK), it replaced mechanical cutting tools called microkeratomes and was utilised for corneal cuts. With pulse energies of several μJ and a 15-kHz pulse frequency, its initial commercial version functioned. In the years that followed, other manufacturers introduced further fs-laser systems for use in corneal surgery. Ziemer FEMTO LDVTM, which debuted a novel strategy combining low pulse energy with high pulse frequencies in 2007, was the pioneer in this field. Another field of ophthalmic fs-laser

application was opened in 2009 with the introduction of the LensX™ system, the first commercially available fs-laser specifically engineered for cataract surgery. Pulses with energy ranging from 6 to 15 μJ and a frequency of 33 kHz were used in the first iterations. After LensX was acquired by Alcon, numerous other companies introduced comparable devices in the years that followed. The Ziemer FEMTO LDV Z8™, the world's first low pulse energy fs laser system for cornea and cataract surgery, hit the market in 2014.

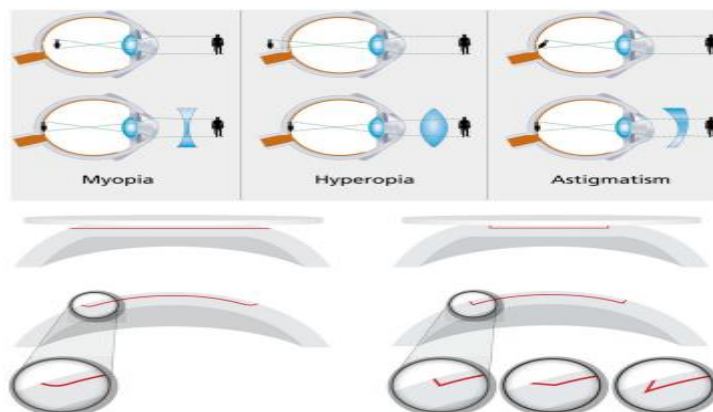


Figure 6: Two types of corneal flaps can be created using the fs-laser technique: (a) a flat, red plane with continuously curved sides that are cut during vacuum docking to a flat interface, and (b) an angled side cut option that takes advantage of 3D cutting geometry.

Clear vision correction

Like a camera's lens, the human eye captures images. A convergent system, primarily made up of the cornea, focuses images on the retina. Myopia and hyperopia are refractive errors that occur when the cornea's curvature and, by extension, its refractive power, do not properly correspond to the eye's axial length. Astigmatism can be corrected through cylindrical correction, corneal flattening, or corneal steepening, all of which are methods of raising or decreasing the cornea's refractive power.

fs Refractive Surgery Flap Creation

The LASIK treatment involves making a flap in the cornea. After lifting the flap, the stromal bed of the cornea can be flattened or steepened using excimer- or solid-state UV-laser radiation, resulting in a change in the cornea's refractive power. Repositioning the flap occurs thereafter. Microkeratomes, mechanical devices, were used to make the flap before fs-laser technology. A variety of patterns can be achieved by using fs-laser technology to complete the flap. Flaps made using fs-(IntraLase™) were shown to have more predictable thickness, improved astigmatic neutrality, and less epithelial injury when compared to flaps made with two different microkeratomes, according to research by Kezirian et al. The researchers Chen et al. verified that flaps made using fs-laser technology are better than microkeratome-cut ones. Flaps for LASIK surgery are now prepared using fs-technology rather than microkeratomes.

Lenticule extraction and intrastromal pockets in the cornea

There are a number of refractive surgery procedures that make use of fs-laser cuts to make "pocket"-shaped holes in the cornea. These holes can then be filled with material or eliminated. The cornea's refractive power changes in both scenarios. Although most ophthalmology fs-associated surgical procedures are just upgrades to older methods, fs-laser technology is the only one that can remove corneal stromal lenticules: in 1994, C. A. Swinger and T. In a patent application, Shui initially detailed the idea of isolating a corneal lamellar disc using a scanned beam of concentrated ultra-short laser pulses. Several groups of German and American scientists worked on the first practical implementations of this novel technique at the same time; in 1999, T. showed it in animal research and laboratory experiments. The crew of Juhasz, then through L. team led by Lubatschowsky. First reported in 2003 [40] were clinical trials in humans with limited vision. In 2007, the first lenticule extraction approach was offered for patients undergoing refractive surgery. This operation utilised a flap incision, similar to LASIK, to openly remove the lenticule from above. is officially known as "FLEx" (Femtosecond Lenticule Extraction). In 2010, a more improved variant was

initially described for clinical usage; this version avoids flap opening and instead employs a short access tunnel incision. It supplanted FLE_x in clinical practice and became famous under the Carl Zeiss Meditec AG brand name SMILE (short incision lenticule extraction). At first, it was solely used to treat nearsightedness, but later on, it was expanded to include myopic astigmatism as well. Later on, competing laser systems for lenticule procedures were introduced by other companies under different names. For example, Schwind's 'SmartSight' and Ziemer Ophthalmic Systems AG's 'CLEAR' (corneal lenticule extraction for advanced refractive correction). This procedure is a laser refractive technique that employs a single femtosecond laser system to create a pocket and dissect a lenticule-shaped piece of tissue inside the corneal stroma. A little incision is made in the access tube to remove the lenticule, which is the contents of the pocket. Consequently, the cornea becomes flatter. Lenticule extraction uses a little arcuate cut of around 90° rather than the larger 270° side cut used in LASIK. That way, a larger portion of the Bowman layer and corneal nerves are spared. Furthermore, less laser energy is required to shape the lenticule as opposed to ablate the same quantity of tissue. Consequently, the lenticule approach may have benefits over conventional LASIK, such as less iatrogenic dry eye, a cornea that is biomechanically stronger after surgery, a smaller incision, and less energy needed to fix refractive errors by laser. On the other hand, surgeons face a more challenging learning curve when it comes to lenticule treatments. Lenticule dissection and extraction was the most challenging stage in Titiyal's analysis of 100 consecutive cases, with a complication frequency of 16% in the first 50 instances with the potential for serious consequences. Five eyes of five patients were studied by Izquierdo lately. The patients had guided lenticule extraction, which involved cutting two incisions with a low-energy femtosecond laser. One incision was made for the anterior plane of the lenticule, while the other was made for the posterior plane. By dividing the area, the dissection plane might be more easily identified, leading to fewer difficulties. The difficulty in curing hyperopia due to the increased curvature, rather than a flattening process, is one drawback of lenticule extraction. In order to implant them into corneas that are either too thin or not stable enough, researchers are currently testing methods of decellularizing and conserving removed lenticules. The refractive outcomes of SMILE were well-predicted, effective, and safe in a prospective randomised paired-eye trial. Given the LASIK procedure's reputation for safety and predictability, it's doubtful that it will demonstrate the superiority of other approaches.

Comprehensive keratoplasty

A corneal button, taken from a deceased donor, is stitched into the recipient cornea during keratoplasty, also known as cornea transplantation. This procedure can be performed either as a full thickness ("penetrating keratoplasty") or as a lamellar keratoplasty, involving only the anterior or posterior layers of the cornea.

Embryo removal

Through the use of donor buttons and a recipient bed that are perfectly congruent, an ideal trephination system is able to provide a tension-free, well-centered fit and effectively waterproof the incision edges. Various trephination systems are currently on the market, including motor-trephine, fs-laser, excimer, and handheld options. The results of comparing motor-trephine with excimer-based trephination reveal that the latter method achieves more precise graft alignment in the recipient bed. Trephination makes it difficult to guarantee accurate centring in the target eye. Thanks to fs Technology's OCT-visualization, limbal oriented centration can be achieved with pinpoint accuracy. Another concern with trephination is the fixation and stabilisation mechanism for the recipient eye and donor button. Any mechanical force acting on the tissue during trephination compresses and distorts it, which in turn decreases the fit between the two. Vacuum suction, applanation, and hybrids of the two are common fixation processes. This advantage could be due to different stabilisation methods; for example, the fs-laser employed in the above trials requires corneal applanation, but excimer laser-assisted keratoplasty does not. Ziemer has devised a novel approach to fs-keratoplasty that uses a liquid optics interface to assist in the cutting of the recipient and donor corneas. This method preserves the cornea's natural curvature during the cutting process. The result is an improvement in donor-receiver congruence and a decrease in tissue shear-and compression artefacts. It will be fascinating to see how fs-trephinations with a liquid optics interface compare to trephinations helped by excimer lasers in the future.

Attacks from the side

A variety of sidecut profiles are available for use in femtolaser aided keratoplasty (FLAK). One possible theoretical benefit is the ability to transplant a proportionally larger number of endothelial cells with a top hat profile. Another is

that it improves the recipient's and donor's vertical and horizontal alignment, which speeds up the healing process and makes the wound more stable. A third is that it preserves the recipient's healthy corneal endothelium. In order to translate these theoretical gains into actual clinical benefits, it is still unclear whether additional elements, including stitching procedures, need to be changed.

Lasik eye surgery

The cornea is made up of five equal layers. On many occasions, the corneal layers are not fully infected. Injuries or infections often leave scars on the outermost layers of skin. Some hereditary corneal illnesses, on the other hand, impact solely the innermost layers of the cornea. Among the many benefits of selectively transplanting the diseased layers is a reduction in transplant rejection due to the reduced amount of tissue being transplanted. Theoretically, two recipients might share a single donor button because to the scarcity of donor material. The eye's structural integrity is unencumbered. Excellent visual outcomes are achievable with manipulation at these levels because to the low amounts of adhesion between the corneal layer interfaces. Approximately 95% of the anterior corneal layers are removed in deep anterior lamellar keratoplasty (DALK), leaving just the innermost layers, the Descemet membrane and the endothelial cell layer. Backwards lamellar keratoplasty, on the other hand, involves removing the cornea's deepest layer—the one that is no longer functioning—and replacing it with the same layer from a donor. In both procedures, fs laser systems aid in the separation of corneal layers at a depth that the patient specifies, facilitating precisely centred, shaped, and sized incisions. In this brief introduction to corneal surgery, we have seen how fs-laser technology offers a vast array of benefits. In a recently published review, the surgical approaches in fs-laser assisted corneal surgery are described in more depth.

Cataract removal procedure

The natural lens is replaced with an artificial intraocular lens (IOL) during cataract surgery because the natural lens becomes less transparent with age. In 2009, Nagy published the first study on fs-laser cataract surgery. Since then, other manufacturers have made rapid advancements in technology and platform capability. Modern, commercially accessible fs systems enable the following procedures to be automated: a) Imaging and measurement of the anterior portion of the eye (including the cornea, anterior chamber, iris, and lens). b) Considering the tissue's dimensions, shape, and position when planning the fs laser cut. c) Corneal incisions, either full-thickness to insert instruments into the eye or partial-thickness to cure astigmatism. d) Removing the lens capsule from the eye via a circular incision (capsulotomy). e) The nucleus of the cataractous lens breaking apart. All of the aforementioned tasks require the use of the aforementioned technology to precisely apply the laser to the desired area and depth by vacuum docking the eye to laser optics. Another review paper by Latz et al. provides a table comparing the main technical parameters of fs laser systems for cataract surgery and other applications. The benefits of fs-assisted cataract surgeries include repeatable and precise laser incisions to the tissue, reduced ultrasound energy used for emulsification (liquification) of the lens nucleus by pre-cutting it into small pieces, pinpoint positioning, length, and depth of corneal incisions, and predictable size and position of capsulotomy. Despite the clear benefits mentioned earlier and multiple studies demonstrating that fs-laser assisted surgery performs better than traditional phacoemulsification manual operation in terms of individual surgical steps, meta-analysis studies were unable to establish overall outcome advantages for fs-laser assisted surgery. However, review papers highlight the benefits of fs-assisted cataract surgery for some patient populations, such as those with low corneal endothelial cell numbers. In regular instances, however, there is no evident advantage of the fs approach over manual phacoemulsification. Intraoperative pupil constriction was one issue with first-generation fs-lasers that was addressed with the advent of low-energy laser ideas.

Endoscopic capsulotomy

Cataract surgery has traditionally involved a continuous curvilinear tugging motion with a needle or forceps to release the anterior lens capsule and provide access to the cataractous lens. The effective lens position, which is a factor in the IOL power, is connected to the size, position, and shape of the capsule opening. After surgery, the eye's refractive error is determined by the power of the intraocular lens (IOL). Problems with intraocular lens tilt, decentration, and increased opacification of the posterior lens capsule might arise from capsular openings that are not sized appropriately. Multifocal, toric, or extended depth-of-focus intraocular lenses (IOLs)—as well as those with other complex optical properties—place a premium on precise lens positioning. Even in difficult circumstances, fs-Lasers

may create well-centered capsular holes (laser capsulotomy) that are precise, predictable, and repeatable. Multiple studies have shown that machines are superior. New intraocular lens (IOL) technologies rely on submillimeter-level precision in capsulotomy size. These innovations make it possible to centre the intraocular lens (IOL) around the capsulotomy instead of the capsular bag.

Fractured lens nucleus

As we age, our lenses become less transparent and flexible, making suction alone ineffective in removing a cataractous lens through a tiny incision. By reducing the amount of ultrasonic energy required for traditional phacoemulsification, femtosecond laser technology makes it possible to pre-cut the nucleus into virtually any shape conceivable. This is beneficial because ultrasonic waves induce oxidative stress, heat, inflammation, and tissue damage.

Tears in the cornea

To insert instruments into the eye, full-thickness incisions in the cornea are required. They are typically made in a variety of sizes using a metal scalpel or diamond blades. Full-thickness corneal incisions can be reliably sized (in terms of width, length, and depth) with the help of fs technology. Astigmatism and iris prolapse might result from the incision site not being properly positioned before surgery. Wounds constructed utilising fs technology are safer, more repeatable, and more stable, according to studies. They also become more watertight. To lessen corneal astigmatism that was present before surgery, partial-thickness incisions are made into the cornea. Improved repeatability and predictability of partial thickness incisions, or even corneal incisions that are entirely intrastromal, are now possible with fs technology. Potentially just as safe and successful as toric intraocular lenses (IOLs) in reducing astigmatism is fs-Laser-assisted corneal incision.

Imaging using Nonlinear Microscopes

Two photon stimulated microscopes were experimentally implemented with the introduction of femtosecond lasers. The two photon absorption is limited to the peak intensity region within the focus of the illuminating laser beam, in contrast to traditional confocal microscopes. High-resolution 3D optical sectioning of thick tissues with minimal bleaching effect or phototoxic effects outside the laser focus is possible with diffraction-limited resolution and depth discrimination without additional pinholes. Using infrared light for multiphoton excitation instead of UV or blue light for 1 photon excited fluorescence (1PEF) allowed for deeper sensing depth with less photodamage effects. Imaging live cells, probing individual molecules, and studying biochemical processes under physiological conditions are all possible with multiphoton excited fluorescence microscopy, thanks to the abundance of nontoxic fluorescent dyes and innovative recording techniques like fluorescence resonant energy transfer (FRET) and fluorescence recovery after photobleaching (FRAP). Images of live cells or photosensitive tissues, such as those in the retina or RPE, were better captured using multiphoton microscopy than using confocal microscopy. A nonlinear laser microscope collects signals from nonlinear optical processes, such as second harmonic generation (SHG) and two-photon excited fluorescence (TPEF), which have recently been used to successfully resolve the fine structure of the collagen fibrils in the cornea and sclera. Due to the spectrum absorbance properties of the cells or tissues, the strength of TPEF-signals is highly affected by the wavelength of the femtosecond laser, in contrast to SHG-signals, which are only weakly excitation-wavelength dependent. There are a number of benefits to using two photon imaging instead of the more conventional single photon imaging method. One is that it eliminates the need for confocal microscopy's additional pinholes, allowing for diffraction-limited resolution and depth discrimination. Important for imaging live cells and tissues, this significantly lessens the likelihood of photodamage or bleaching effects outside the laser's focus. In order to get a large sensing depth with minimal photo-damage, it is possible to use infrared (IR) lasers instead of UV or blue light stimulation. (4) Since the human cornea is impermeable to ultraviolet light, spectral imaging of the living retina becomes possible with the use of infrared light, which is comparable to UV light with a single photon.

Image Analysis of Collagen Fibrils in the Cornea, Sclera, and Optic Nerve Head using Second Harmonic Generation Imaging

The distinctive physiological and visual features of the connective tissues, such as the cornea and sclera, are determined by collagen, the most abundant protein in the human body. Collagen fibrils in ocular tissue have a

noncentrosymmetric structure, which allows SHG imaging to explore their fine structure. Previously, this structure could only be resolved by light or electron microscopy following complex tissue preparation. Obtaining high-resolution, highly contrast, and extensive sensing depth images of the untreated corneal and scleral tissue is possible without the need for staining, fixation, or slicing [25,26]. Using SHG imaging, the corneal collagen fibre structure of a human donor eye may be seen clearly. Observations of two distinct collagen fibre distributions were made in relation to the scan's depth. Short, tiny, and disorganised collagen fibres made up the anterior Bowman's membrane. Collagen fibres in the corneal stroma showed impressive uniformity and the characteristic undulation. Along the corneal surface, they ran in a highly organised and tightly packed fashion. Although there are a small number of areas where neighbouring domains have nearly perpendicular fibre orientation, the orientation of the majority of collagen fibres is consistent with its neighbours. This finding is in perfect agreement with the well-known histological features of the cornea, which normally necessitate invasive sample preparations. The shape and size of the collagen fibrils are reflected in the geometry of the SHG emission field, which is one of the distinctive properties of SHG. The phase matching condition causes the SHG emission from the collagen fibril to be extremely asymmetrical, in contrast to the fluorescence signal. Objects with an axial size around the second harmonic wavelength show forward directed SHG, according to earlier theoretical and experimental studies. On the other hand, objects with an axial size below $\lambda/10$ (approx. 40nm) are predicted to generate almost equal amounts of backwards and forward SHG signals. The cornea's backwards SHG was quite weak, as shown in. Consistent with prior electron microscopy results and theoretical modelling of cornea transparency, the preponderant forward SHG suggests that the corneal collagen fibrils are consistently structured as a polycrystalline film, rather than randomly distributed. This startling fact was proven here. despite the fact that the strength of the forward SHG is comparable to that of the backwards SHG from the sclera. Consistent with prior research on tendon collagen fibrils, the scleral collagen microfibrils produce uniformly dispersed forward and backwards SHG due to their well-aligned shell (thickness less than 40 nm) and their randomly-arranged core. In order to keep the sclera's high rigidity and elasticity, the irregular, tube-like scleral fibrils might be useful. Elevated intraocular pressure (IOP) is a hallmark of glaucoma, an optic neuropathy. While the exact role of intraocular pressure (IOP) in glaucoma development and progression is still up for debate, it is believed that aberrant strain and stress on the ONH connective tissue caused by high IOP may exacerbate damage to neuronal axons. The connective tissues of the ONH lamina cribrosa have only been studied in vivo using fundus cameras or confocal SLO, neither of which have sufficient resolution to reveal the deformation of the lamina cribrosa with a particular depth resolution. Our findings demonstrate that SHG imaging can reveal the submicron-scale organisation of collagen fibres in the ONH, which is particularly intriguing given that collagen is the predominant protein in the lamina cribrosa. Methods such as confocal SLO, retina angiography, and TPEF imaging of blood vessels can be used to quantitatively and spatially exclude abnormalities in the lamina cribrosa, optic nerve vascular nutrition, and intraocular pressure (IOP).

Magnification of Lipofuscin Granules in Red Blood Cells by Two-Photon Autofluorescence Imaging

The leading cause of permanent vision loss and documented cases of legal blindness among the elderly in developed nations is age-related macular degeneration (AMD). In context, consider that 35% of the population over 75 has AMD to varying degrees. Retinal pigment epithelium (RPE), choroid, and retinal degeneration all proceed together in AMD. The buildup of drusen, a watery substance, between the retinal pigment epithelium (RPE) and the choroid is the first outward aberration in age-related macular degeneration (AMD). An aberrant increase in autofluorescence (AF) from RPE cells has been linked to drusen development in prior research. As a result of intracellular digestion, the lipofuscin granule contains the fluorophores that are most prominent in RPE AF. Retinal pigment epithelial cells (RPE) are vulnerable to damage from excessively accumulated lipofuscin granules, which cause retinal degeneration. To better understand the biological basis of AMD's early development and to create more sensitive ophthalmic diagnostic methods based on microscopic autofluorescence imaging of RPE cells, this imaging technique is crucial. Confocal microscopes have long been the tool of choice for high-resolution fluorescent imaging of RPE cells. Multiphoton microscopic imaging of RPE cells from the human eye has not been reported yet, despite the fact that TPEF imaging is well suited to characterise RPE cell autofluorescence (more sensing depth, better resolution, less photon damage). When compared to confocal imaging, TPEF imaging yields higher quality results, as shown in. The distribution of lipofuscin granules within RPE cells and the appearance of individual RPE cells were both visualised with submicron resolution. There was no unwanted photo bleaching or photodamage caused by TPEF when the excitation strength was 4 mW. Because the lipofuscin granules are localised to the space between the cell membrane and the nucleus, high-

resolution, highly contrast images reveal the precise position and form of the RPE cells. There was a regular hexagonal arrangement of densely packed RPE cells in the macula. Despite lipofuscin granules usually having a diameter smaller than $1\mu\text{m}$, confocal and TPEF imaging are able to resolve the lipofuscin granule boundaries. Confocal imaging with 488 nm Argon laser excitation makes lipofuscin granules in the centre of RPE cells almost invisible; however, TPEF imaging using an effective excitation wavelength of 400 nm can show more of them. With a dominant autofluorescence emission at $\lambda > 560\text{ nm}$, the autofluorescence of lipofuscin granules excited by a single photon appears yellow-red, in agreement with earlier studies ([30,31]). But when excited with two photons, green autofluorescence in the 500–550 nm band becomes noticeable. The macula displays a consistent arrangement of RPE cells in a hexagonal packing pattern, as demonstrated in. There is a wide range of morphologies and sizes among RPE cells in the retina's periphery. Lipofuscin granules are seen in the space between the cell membrane and the nucleus, but there is no evidence that they can cross the membrane of RPE cells. Some peripheral RPE cells even showed signs of having two nuclei in their expanded forms. An 80-year-old patient's macula RPE cells showed aberrant lipofuscin granules, as shown in TPEF imaging. There was an increase in the blue-green fluorescence of these aberrant lipofuscin granules. I should note that compared to normal granules, the majority of the abnormal ones seemed to be much larger, with a diameter exceeding $2\mu\text{m}$. Nevertheless, aberrant lipofuscin granule-containing RPE cells were extremely uncommon (less than 1%) in comparison to the vast majority of normally functioning RPE cells. Isolated RPE cells contained the vast majority of the aberrant lipofuscin granules. The distinct spectrum that was detected could not have been caused by a manufacturing error or contamination in the samples because there was no sign of cell membrane damage.

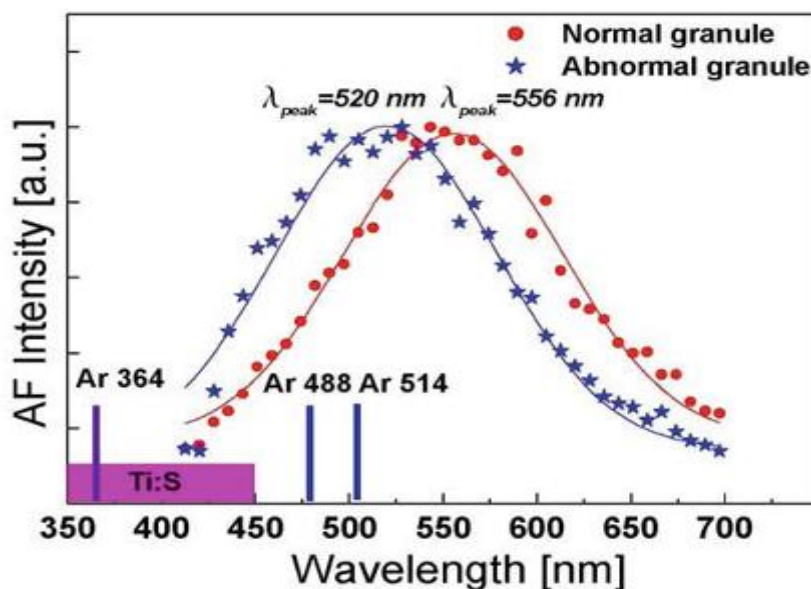


Figure 7. Using 10 nm increments, a photomultiplier detector measured autofluorescence (AF) signals, which were then fitted using Gaussian functions. Abnormal lipofuscin granules' AF spectra are represented by the blue stars, whereas normal granules' AF spectra are represented by the red circles.

The autofluorescence spectra of RPE cells seemed better characterised using TPEF imaging, which also has the advantages of a large sensing depth and less photodamage. The full autofluorescence spectrum could not be excited by the usual blue Argon laser emission line ($\lambda = 488,514\text{nm}$). With femtosecond IR beam excitation, the full spectrum of autofluorescence may be studied, thanks to the wide tuneable excitation source (Ti:Sapphire laser, $\lambda = 720\text{-}980\text{nm}$) for TPEF imaging, which encompasses both UV and blue excitation ($\lambda = 360\text{-}490\text{nm}$). The molecular fingerprint of lipofuscin, which is a green-blue shifted autofluorescence, suggests the existence of aberrant proteins or fluorophores within the granules. This could be a result of the host RPE cells' disrupted metabolic process during the early stages of AMD.

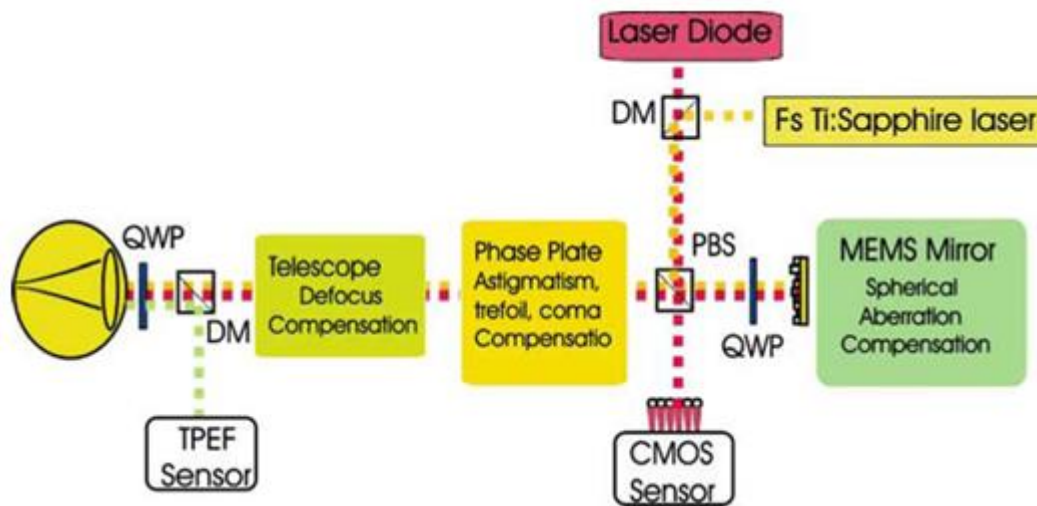


Figure 8. System for adaptive optics that allows for aberration-free imaging of the retina. DM stands for dichroic mirror; QWP for quarter-wave-plate; and PBS for polarising beam splitter. A two-photon-excited-fluorescence (TPEF) system Mikro-electro-mechanical-system (MEMS); the complementary metal-oxide-semiconductor Shack-Hartmann wavefront sensor.

Conclusion

We have shown that ultrafast femtosecond lasers offer great promise for use in ophthalmic surgery. Utilising the distinct characteristics of the laser-tissue interaction process in the femtosecond time domain, laser flap cuts (LMK) for intrastromal refractive operations and excimer LASIK can achieve optimal results. Another area that could benefit from ultrafast lasers in ophthalmic surgery is glaucoma treatment, which involves creating tiny canals within the eye to alleviate pressure inside the eye. The development of ultrafast laser technology has obviously progressed to the point where practical ophthalmic applications can optimise the utilisation of the extremely brief laser pulses. We will be able to aid patients who are currently untreatable with traditional surgical techniques thanks to some of the described uses. There are new ways to attain supernormal vision, and these use wavefront-based tailored surgical methods. Novel developments utilising SHG- and TPEF-imaging have been documented in relation to nonlinear imaging of intraocular structures with femtosecond laser illumination. In addition to its potential use in basic research on collagen fibrils or their collagen equivalents, SHG imaging has potential clinical applications in the early detection of corneal-related disorders and the precise monitoring of tissue repair following refractive surgery. Backwards SHG imaging could be a sensitive way to examine cornea haze or cloudiness, when the regularity of the collagen fibrils is altered, clinically, even though forward SHG imaging doesn't seem to be practical for diagnostic purposes. Imaging of RPE cells with 1PEF and 2PEF allowed for submicron resolution visualisation of cellular shape and distribution of lipofuscin granules. While most RPE cells have lipofuscin granules with a diameter less than $1\mu\text{m}$, a small percentage (less than 1%) have granules with a diameter greater than $2\mu\text{m}$. Interestingly, these aberrant or gigantic lipofuscin granules exhibited heightened blue-green fluorescence. The blue-shifted autofluorescence of lipofuscin, which serves as a chemical fingerprint of the substance, suggests the existence of aberrant proteins or fluorophores within the granules. These could be a result of the host RPE cells' disrupted metabolic process. It seems that TPEF imaging of the living retina is especially useful for diagnostic and pathological research of RPE-related eye illnesses, according to a suggested two-photon laser scanning ophthalmoscope with adaptive-optical beam shaping.

References

1. L. Zickler, M. Han, G. Giese, F. Loesel, J. Bille, Proceedings of The International Society for Optical Engineering (SPIE) 4978, 194–207 (2003) 3 Femtosecond Lasers in Ophthalmology 73 10. G. Mourou, Appl. Phys. B 65, 205–211 (1997)

2. M. Kaschke, K.-H. Donnerhacke, and M. S. Rill, *Optical Devices in Ophthalmology and Optometry: Technology, Design Principles and Clinical Applications*, Weinheim, WILEY-VCH Verlag GmbH & Co. KGaA, 2014.
3. C. Latz, T. Asshauer, C. Rathjen, and A. Mirshahi, "Femtosecondlaser assisted surgery of the eye: overview and impact of the lowenergy concept," *Micromachines*, vol. 12, no. 2, 2021.
4. R. Bhargava, P. Kumar, H. Phogat, and K. P. Chaudhary, "Neodymium-yttrium aluminium garnet laser capsulotomy energy levels for posterior capsule opacification," *J. Ophthalmic Vis. Res.*, vol. 10, no. 1, pp. 37–42, 2015.
5. A. Vogel, J. Noack, G. Hüttman, and G. Paltauf, "Mechanisms of femtosecond laser nanosurgery of cells and tissues," *Appl. Phys. B*, vol. 81, no. 8, pp. 1015–1047, 2005.
6. A. Heisterkamp, T. Ripken, H. Lubatschowski, E. Lütkefels, W. Drommer, and W. Ertmer, "Intrastromal cutting effects in rabbit cornea using femtosecond laser pulses," in *Optical Biopsy and Tissue Optics*, vol. 4161, Bellingham, SPIE, 2000, pp. 52–60.
7. A. Vogel, R. Busch, and U. Parlitz, "Shock wave emission and cavitation bubble generation by picosecond and nanosecond optical breakdown in water," *J. Acoust. Soc. Am.*, vol. 100, no. 1, pp. 148–165, 1996.
8. V. Venugopalan, "Mechanisms of pulsed laser ablation of biological tissues," *Chem. Rev.*, vol. 103, no. 2, pp. 577–644, 2003.
9. N. Tinne, G. Knoop, N. Kallweit, et al., "Effects of cavitation bubble interaction with temporally separated fs-laser pulses," *J. Biomed. Opt.*, vol. 19, no. 4, p. 048001, 2014.
10. H. Lubatschowski, G. Maatz, A. Heisterkamp, et al., "Application of ultrashort laser pulses for intrastromal refractive surgery," *Graefes Arch. Clin. Exp. Ophthalmol.*, vol. 238, no. 1, pp. 33–39, 2000
11. F. Loesel, J. Fischer, M.G"otz, C. Horvarth, T. Juhasz, F. Noack, N. Suhm, J. Bille, *Appl. Phys. B* 66, 121–128 (1998)
12. F. Loesel, L. Zickler, R. Kessler, in *Refractive Surgical Applications of Ultra short Pulse Lasers*, ed by J. Bille, C. Harner, F. Loesel, *New Frontiers in Vision and Aberration-Free Refractive Surgery*, 1st ed.(Springer, Berlin Heidelberg New York, 2003), p. 159–175
13. T. Juhasz, F. Loesel, R. Kurtz, C. Horvath, J.F. Bille, G. Mourou, *IEEE J. Quant. Electron.* 5, 902–910 (1999)
14. Heisterkamp, T. Ripken, E. L'utkefels, W. Drommer, H. Lubatschowski, W. Welling, W. Ertmer, *Ophthalmologie* 98, 623–628 (2001)
15. T. Juhasz, F. Loesel, C. Horvath, R. Kurtz, G. Mourou, *Ultrafast Phenomena*, 42–43 (1998) 16. M. Hamill, T. Kohlen, *J. Cataract. Refract. Surg.* 28, 328–336 (2002)
16. R. Kurtz, G. Spooner, K. Sletten, K. Yen, S. Sayegh, F. Loesel, C. Horvath, H. Liu, V. Elnor, D. Cabrera, M.-H. Meunier, Z. Sacks, T. Juhasz, D. Miller, A. Williams, *Proceedings of the SPIE* 3616, 51–65 (1999)
17. W. Denk, J. Strickler, W. Webb, *Science* 248, 73–76 (1990) 20. W. Zipfel, R. Williams, W. Webb, *Nat. Biotechnol.* 21, 1369–1377 (2003)
18. B. Masters, *Selected papers on multiphoton excitation microscopy*, Milestone Series MS 175, (Bellingham, WA: SPIE Optical Engineering Press, 2003)
19. A. Yeh, N. Nassif, A. Zoumi, B. Tromberg, *Opt. Lett.* 27, 2082–2084 (2002) 23. M. Han, L. Zickler, G. Giese, M. Walter, J. Bille, *Microscopic Evaluation of Femtosecond Laser Intrastromal Surgery*. *Proceedings of The International Society for Optical Engineering (SPI)*, Munich 5142, 127–136 (2003)
20. J. Bille, C. Harner, F. Loesel, *New Frontiers in Vision and Aberration-Free Refractive Surgery*, 2nd edn. (Springer, Berlin Heidelberg New York, 2003)

21. J. S. Pepose and H. Lubatschowski, "Comparing Femtosecond Lasers," *Cataract Refract. Surg. Today*, pp. 45–51, 2008.
22. I. Ratkay-Traub, T. Juhasz, C. Horvath et al., "Ultra-short pulse (femtosecond) laser surgery: initial use in LASIK flap creation," *Ophthalmol. Clin. North Am.*, vol. 14, no. 2, pp. 347–355,
23. Z. Nagy and C. McAlinden, "Femtosecond laser cataract surgery," *Eye Vis.*, vol. 2, p. 11, 2015.
24. H. Lubatschowski, "Overview of commercially available femtosecond lasers in refractive surgery," *J. Refract. Surg.*, vol. 24, no. 1, pp. S102–S107, 2008.
25. A. K. Riau, Y. C. Liu, N. C. Lwin, et al., "Comparative study of nJ and μ J-energy level femtosecond lasers: evaluation of flap adhesion strength, stromal bed quality, and tissue responses," *Invest. Ophthalmol. Vis. Sci.*, vol. 55, no. 5, pp. 3186–3194, 2014.
26. W. J. Mayer, O. K. Klaproth, M. Ostovic, et al., "Cell death and ultrastructural morphology of femtosecond laser-assisted anterior capsulotomy," *Investig. Ophthalmol. Vis. Sci.*, vol. 55, no. 2, pp. 893–898, 2014.
27. T. Schultz, S. C. Joachim, M. Stellbogen, and H. B. Dick, "Prostaglandin release during femtosecond laser-assisted cataract surgery: main inducer," *J. Refract. Surg.*, vol. 31, no. 2, pp. 78–81, 2015.
28. A. Vogel, "Energy balance of optical breakdown in water at ns to fs time scales," *Appl. Phys. B*, vol. 68, no. 2, pp. 271–280, 1999.
29. J. H. Talamo, P. Gooding, D. Angeley, et al., "Optical patient interface in femtosecond laser-assisted cataract surgery: contact corneal appplanation versus liquid immersion," *J. Cataract Refract. Surg.*, vol. 39, no. 4, pp. 501–510, 2013.
30. A. F. Fercher, W. Drexler, C. K. Hitzenberger, and T. Lasser, "Optical coherence tomography – principles and applications," *Rep. Prog. Phys.*, vol. 66, no. 2, pp. 239–303, 2003.
31. J. S. Schuman, C. A. Puliafito, J. G. Fujimoto, and J. S. Duker, *Optical Coherence Tomography of Ocular Diseases*, New Jersey, Slack Inc., 2012.
32. A. F. Fercher, K. Mengedoht, and W. Werner, "Eye-length measurement by interferometry with partially coherent light," *Opt Lett.*, vol. 13, no. 3, pp. 1867–1869, 1988.
33. M. Wojtkowski, R. Leitgeb, A. Kowalczyk, T. Bajraszewski, and A. F. Fercher, "In vivo human retinal imaging by Fourier domain optical coherence tomography," *J. Biomed. Opt.*, vol. 7, no. 3, pp. 457–463, 2002.
34. O. Kermani, W. Fabian, and H. Lubatschowski, "Real-time optical coherence tomography-guided femtosecond laser sub-Bowman keratomileusis on human donor eyes," *Am. J. Ophthalmol.*, vol. 146, no. 1, pp. 42–45, 2008.
35. R. Ambrosio, Jr., B. F. Valbon, F. Faria-Correia, I. Ramos, and A. Luz, "Scheimpflug imaging for laser refractive surgery," *Curr. Opin. Ophthalmol.*, vol. 24, no. 4, pp. 310–320, 2013.
36. M. Shajari, S. Khalil, G. Al-Khateeb, et al., "Comparison of 2 laser fragmentation patterns used in femtosecond laser-assisted cataract surgery," *J. Cataract Refract. Surg.*, vol. 43, no. 12, pp. 1571–1574, 2017.
37. D. S. Grewal, T. Schultz, S. Basti, and H. B. Dick, "Femtosecond laser-assisted cataract surgery—current status and future directions," *Surv. Ophthalmol.*, vol. 61, no. 2, pp. 103–131, 2016.
38. D. Aron-Rosa, J. J. Aron, M. Griesemann, and R. Thyzel, "Use of the neodymium-YAG laser to open the posterior capsule after lens implant surgery: a preliminary report," *J. Am. Intraocul. Implant. Soc.*, vol. 6, no. 4, pp. 352–354, 1980.
39. Z. Nagy, A. Takacs, T. Filkorn, and M. Sarayba, "Initial clinical evaluation of an intraocular femtosecond laser in cataract surgery," *J. Refract. Surg.*, vol. 25, no. 12, pp. 1053–1060, 2009.
40. G. M. Kezirian and K. G. Stonecipher, "Comparison of the IntraLase femtosecond laser and mechanical keratomes for laser in situ keratomileusis," *J. Cataract Refract. Surg.*, vol. 30, no. 4, pp. 804–811, 2004.

41. S. Chen, Y. Feng, A. Stojanovic, M. R. Jankov, 2nd, and Q. Wang, "IntraLase femtosecond laser vs mechanical microkeratomes in LASIK for myopia: a systematic review and meta-analysis," *J. Refract. Surg.*, vol. 28, no. 1, pp. 15–24, 2012.
42. C. A. Swinger and T. L. Shui, *Method of Performing Ophthalmic Surgery*, Patent WO9409849A1, 1994.
43. T. Juhasz, F. H. Loesel, R. M. Kurtz, C. Horvath, J. F. Bille, and G. Mourou, "Corneal refractive surgery with femtosecond lasers," *IEEE J. Sel. Top. Quant. Electron.*, vol. 5, no. 4, pp. 902–910, 1999.
44. I. Ratkay-Traub, I. E. Ferincz, T. Juhasz, R. M. Kurtz, and R. R. Krueger, "First clinical results with the femtosecond neodymium-glass laser in refractive surgery," *J. Refract. Surg.*, vol. 19, no. 2, pp. 94–103, 2003 [
45. W. Sekundo, K. Kunert, C. Russmann, et al., "First efficacy and safety study of femtosecond lenticule extraction for the correction of myopia: six-month results," *J. Cataract Refract. Surg.*, vol. 34, no. 9, pp. 1513–1520, 2008.
46. W. Sekundo, K. S. Kunert, and M. Blum, "Small incision corneal refractive surgery using the small incision lenticule extraction (SMILE) procedure for the correction of myopia and myopic astigmatism: results of a 6 month prospective study," *Br. J. Ophthalmol.*, vol. 95, no. 3, pp. 335–339, 2011.
47. R. Shah, "History and results; indications and contraindications of SMILE compared with LASIK," *Asia Pac. J. Ophthalmol.*, vol. 8, no. 5, pp. 371–376, 2019.